Development of a method to achieve antegrade in situ fenestration of endovascular stent grafts in abdominal aortic aneurysms

Cyrus J. Darvish, BS,[a] Nicholas P. Lagerman, MS,[a] Oldrich Virag, BS,[a] Hannah Parks, BS,[a] Yash K. Pandya, MD,[b] Mohammad H. Eslami, MD,[c] David A. Vorp, PhD,[a,d,e,f,g,h,i,j,k] *and* Timothy K. Chung, PhD,[a,h] *Pittsburgh, PA; and Charleston, WV*

ABSTRACT

Abdominal aortic aneurysm (AAA) is the focal dilation of the terminal aorta, which can lead to rupture if left untreated. Traditional endovascular aneurysm repair techniques are minimally invasive and pose low mortality rates compared with open surgical repair; however, endovascular aneurysm repair procedures face challenges in accommodating variations in the patient's anatomy. Complex aneurysms are defined when the sac extends past the renal arteries or has an insufficient neck landing zone to deploy a traditional endograft. Fenestrated endografts were introduced to enable the repair of complex aneurysms by the creation of fenestrations to enable blood flow into the visceral arteries. This study investigates proof of concept for creating antegrade in situ fenestrations of off-the-shelf endografts using a novel endovascular orifice detection device. Our technique enables the precise location of the visceral artery orifices using fiber optic cables and an infrared light source. The endovascular orifice detection device was tested rigorously in precisely locating an artery opening in blood and a custom AAA phantom model. The study also explored the safest means of creating a fenestration using mechanical puncture and a laser. This innovative approach offers a viable alternative for patients with complex AAAs. (J Vasc Surg Cases Innov Tech 2025;11:101661.)

Keywords: Abdominal aortic aneurysm; Complex abdominal aortic aneurysm; Endovascular repair; FEVAR; Laser fenesttr; In-situ fenestration of endografts

An abdominal aortic aneurysm (AAA) is a localized enlargement of the terminal aorta by >50%[1] that can rupture, leading to massive, life-threatening internal bleeding.[2] AAA rupture is the 13th leading cause of death in the United States for people >65 years of age.[1] Current procedures[3] for preventing rupture are costly and include vigorous monitoring of the aneurysm until the diameter reaches a critical threshold of 4.5 to 5.0 cm for women and 5.0 to 5.5 cm for men.[4] Once this diameter is met, surgical intervention is often recommended to avoid the risk of AAA rupture.[5]

Current methods to repair a AAA include open repair[6] or minimally invasive endovascular aneurysm repair (EVAR).[7,8] Roughly 30% to 50% of patients with AAAs are not eligible for EVAR owing to the complexity of their aneurysm anatomy, such as short necks or insufficient sealing zones for the endograft.[9] Fenestrated endovascular aneurysm repair (FEVAR) was introduced to accommodate a wide range of complex geometry aneurysms that are either physician modified (PMEG)[10] or custom manufactured devices (CMD).[11] Currently, only one US Food and Drug Administration-approved CMD, the Cook Zenith graft (Cook Medical LLC, Bloomington, IN), is on the market.[12] Owing to the complexity of manufacturing these grafts, patients have waiting times of 6 weeks on average, with ≤12 weeks in some cases.[13,14] This delay can lead to an increased chance of aneurysm rupture and death.[15,16] A recent study highlighted the risk of surgical delay by reporting that 4.1% of patients died, 1.7% experienced aneurysm rupture, and 0.1% required emergency rupture repair waiting for elective repair.[15] While PMEGs provide an alternative to CMDs, they require an investigational device exemption from the FDA, making them unavailable in several institutions. They also requrie significant pre-planning that can lead to long operating times.[17]

In situ fenestration (ISF) of AAA endografts is a sophisticated technique that has shown great promise.[18-20] It involves creating openings in the graft once it is already placed inside the aorta. The two primary methods for fenestrations are retrograde, meaning fenestration of the graft from the visceral artery side, or antegrade, from inside the lumen of the aortic graft.[21] The means

From the Department of Bioengineering, University of Pittsburgh[a]; the School of Medicine, University of Pittsburgh Medical Center,[b] Pittsburgh; the Department of Surgery, West Virginia University, Charleston; [c]Department of Surgery,[d] McGowan Institute for Regenerative Medicine,[e] Department of Chemical and Petroleum Engineering,[f] Department of Cardiothoracic Surgery,[g] Clinical & Translational Sciences Institute,[h] Department of Mechanical Engineering and Materials Science,[i] Center for Vascular Remodeling and Regeneration,[j] and Magee Women's Research Institute,[k] University of Pittsburgh, Pittsburgh.

D. A. V. and T. K. C. contributed equally to supervising work.

Correspondence: Timothy K. Chung, PhD, Department of Bioengineering, Swanson School of Engineering, University of Pittsburgh, Research Assistant Professor, 300 Technology Dr, Ste 413, Center for Bioengineering, Pittsburgh, PA 15213 (e-mail: tkc12@pitt.edu).

2468-4287

https://doi.org/10.1016/j.jvscit.2024.101661

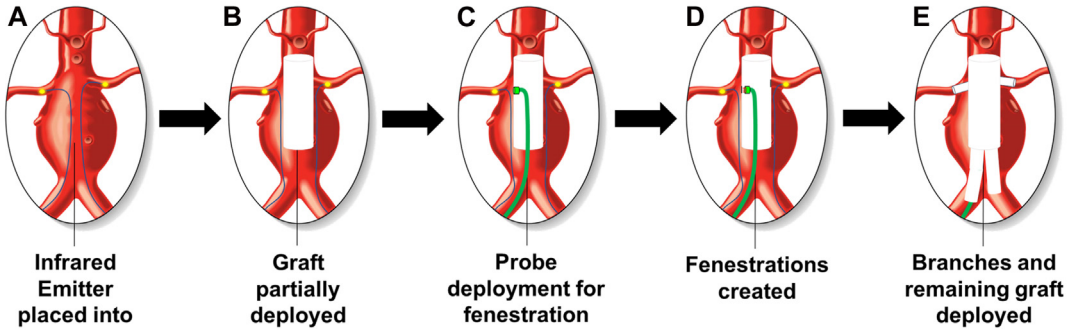

Fig 1. A brief overview of how the endovascular orifice detection (EOrD) device will be deployed clinically, starting with **(A)** infrared emitters placed into the visceral arteries, **(B)** the endograft is deployed partially, temporarily covering the arteries, **(C)** deployment of EOrD device to target the precise location of the target vessels through the endograft, **(D)** perform fenestration through the endograft, and pass a guide wire through the fenestration while removing the emitter from the target vessel. **(E)** Lastly, deploy the branching stents through the target vessels.

of creating the hole are either mechanical (eg, punctured with a needle) or via a laser, where a small probe burns through the graft to create a laser fenestration.[22] However, one of the predominant challenges in this procedure is locating the visceral arteries accurately, specifically in antegrade ISF. At present, there are no FDA approved devices for ISF. Clinicians can perform ISF by pre-cannulating the branching vessels and pre-stenting the vessel.

In this article, we present a novel approach to detect the openings of visceral arteries using infrared emitters and receivers. The endovascular orifice detection (EOrD) device is a intended for visualizing the orifice of an artery in real time and three-dimensional (3D) space, enabling potentially more accurate fenestrations in traditonal off-the-shelf endografts (Fig 1, *A-E*) and eliminating the wait time for CMDs and PMEGs. This study aims to assess the feasibility of locating an artery in real time using infrared light for laser fenestration in an in vitro AAA phantom while also comparing the safety between mechanical and laser fenestration techniques.

METHODS

The overall procedure for deploying the EOrD device clinically begins with advancing light emitters into the target branching vessels via femoral access. Next, an off-the-shelf main body endograft is deployed in the affected area. Once the main body graft is deployed, the EOrD device is advanced through the endograft via femoral access to locate the target vessels by detecting an emitter. After the target vessel is located, a fenestration is created, and a guide wire is passed through the fenestration and into the target vessel.

Visualization using fiber optics. We first explored whether fiber optics are a feasible modality for locating an artery opening and whether fiber optics can detect light through blood. A two-part cast for silicone molding was designed using Autodesk Inventor (Autodesk, San Rafael, CA) and 3D printed using a Form 3 printer (Formlabs, Somerville, MA). The probe head was designed to have a 7 mm diameter, containing six 0.50 numerical aperture, 740-μm diameter fiber optic cables (Thorlabs, Newtown, NJ), arranged in a 6 mm diameter, radially spaced every 60°. Six cables were chosen as an optimal number for clear visualization while ensuring efficient use of equipment. A 10:1 XPS silicone (Silicones Inc., Woodbine High Point, NC) was blended, poured into the cast, and left to dry. The final mold can be seen in Fig 2, *A*.

For visualization, the free ends of the cables were threaded through a 3D printed disk in the same arrangement as the probe head. This disk was then affixed to a cylindrical tube to eliminate ambient light for optimal viewing of infrared light. A webcam (Logitech International, Lausanne, Switzerland) was set up on the opposite end of the tube to record the light captured by the cables.

A test bench was designed and 3D printed for an experiment using chelated sheep blood (Fig 2, *B*). In the center was a half-cylinder, representing the inside of the lumen to the outer wall. Guide rails were integrated on both sides of this half-cylinder to facilitate smoother probe navigation while immersed in blood. A 6-mm hole in the center simulated an arterial opening. A piece of Zenith graft material was trimmed and glued on the hole's surface. Through the back, an infrared LED was affixed to the opening.

For testing, the head of the probe was placed on one edge of the artery opening and swept across the face of the hole while maintaining a constant distance of 3 mm from the glued-on graft. Comparative tests were conducted in both air and chelated sheep blood (Lampire Biological Lab, Pipersville, PA) to discern light dissipation caused by blood. A MATLAB script captured images of the light transmitted by the cables (Fig 2, *C*), which were subsequently converted to 8 bit grayscale ranging

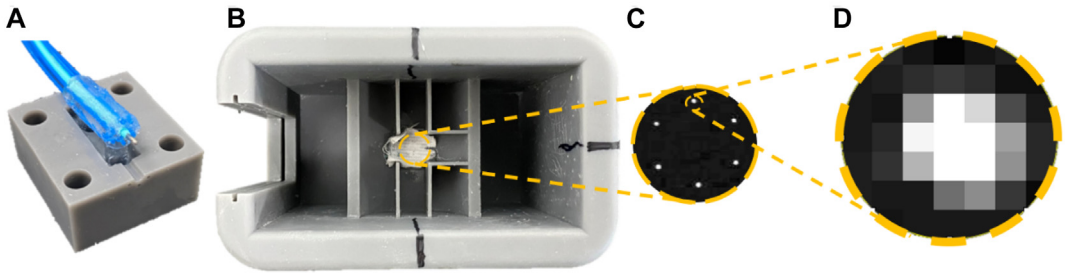

Fig 2. (A) Silicone probe in half of the 3D printed cast with six fiber optic wires embedded. **(B)** Test chamber with endograft material glued over a hole opening in the center with an emitter placed inside. **(C)** Visualization of the probe tip over the center of the opening from the MATLAB code. **(D)** A fixed area was created over an individual fiber for intensity measurement using ImageJ.

in value from 0 to 255. A single snapshot was then isolated while the probe was over the center of the opening for both air and blood. The grayscale values from both shots were analyzed using ImageJ (National Institutes of Health, Bethesda, MD). A comprehensive analysis was undertaken on all six cables, noting average and peak grayscale values within a predefined region. This examination zone is referred to as the area of intensity (Fig 2, *D*).

In vitro test bench and AAA phantom. Several juxtarenal AAA models were molded out of silicone using the split-molding technique previously described in Visualization using fiber optics (Fig 3, *A* and *B*) for assessing the deployment of the device in an in vitro setting. A dissolving inner core, made from polyvinyl alcohol, was 3D printed (Flashforge, Zhejiang, China) for the lumen of the AAA mold. The dimensions of the AAA model were 14.5 cm long, 8.5 cm wide (renal opening to renal opening), an aortic lumen diameter of 26 mm, a renal lumen of 6.35 mm, and an iliac lumen of 19 mm. A custom 1/4″ thick acrylic (McMaster Carr, Elmhurst, IL) chamber was designed and manufactured using a 50-W laser cutter (OMTech, Anaheim, CA). The acrylic enclosure was designed to fit the AAA phantom and accommodate tubing connecting the phantom to a pulsatile flow loop for circulating blood and water (Fig 3, *C*).

Measuring factor of safety for mechanical puncture method of fenestration. A test was designed to investigate the safest method for fenestration, mechanical or laser. The differences between these procedures were determined through compression testing and imaging.

For mechanical fenestration, a custom clamping piece was 3D printed to hold a section of porcine aorta for needle compression. A one-newton spring weight was attached to an end of the specimen to hold taut at a consistent force. A second 3D printed piece was designed to hold a 20 gauge needle to remove potential movement during testing. For this test, a 32 mm square section was cut from the porcine aorta, and a piece of Cook Zenith graft material was cut with the same dimensions. The 3D printed piece holding the porcine aorta was attached to the bottom pneumatic clamp of an Instron 5543A testing machine (Instron Inc., Norwood, MA). The second piece holding the needle was attached to the top pneumatic clamp. A mechanical puncture test was then performed at a 3 mm/minute-controlled rate until the needle punctured the material thoroughly. The test was performed on three configurations: endograft material alone (n = 5 locations), porcine aorta alone (n = 3 locations), and combined endograft on top of the aorta (n = 3 locations). The maximum puncture force was recorded for each test, and the factor of safety was calculated between the peak force of the combination of the endograft and porcine aorta with the endograft and aorta alone using the following equation:

$$Factor\ of\ Safety = \frac{f_{failure}}{f_{working}}$$

Where the *Factor of safety* is defined as the ratio of failure force ($f_{failure}$) or maximum failure force (in this case, the combination of endograft and aorta) to the working force ($f_{working}$) or the maximum force for the aortic wall. Calculating the factor of safety in this way determines how adding an endograft will help to mitigate potential damage to the aorta during fenestration. A value of 1 would indicate the endograft and aorta would be pierced at the same time, making mechanical puncture dangerous. A value of >1 indicates that there is a threshold of puncture before the needle breaks through to the aorta.

Laser fenestration was performed using a CVX-300 Excimer Laser System (Phillips Inc., Amsterdam, the Netherlands). The laser was used on sections of the endograft attached to the porcine aorta. The test was performed on two different endografts: a Medtronic endograft and a Zenith endograft. The laser was pulsed on the combination of endograft and aorta using 1-, 2-, 3-, and 4-second pulses at a fluence of 60 mJ/mm^2 and

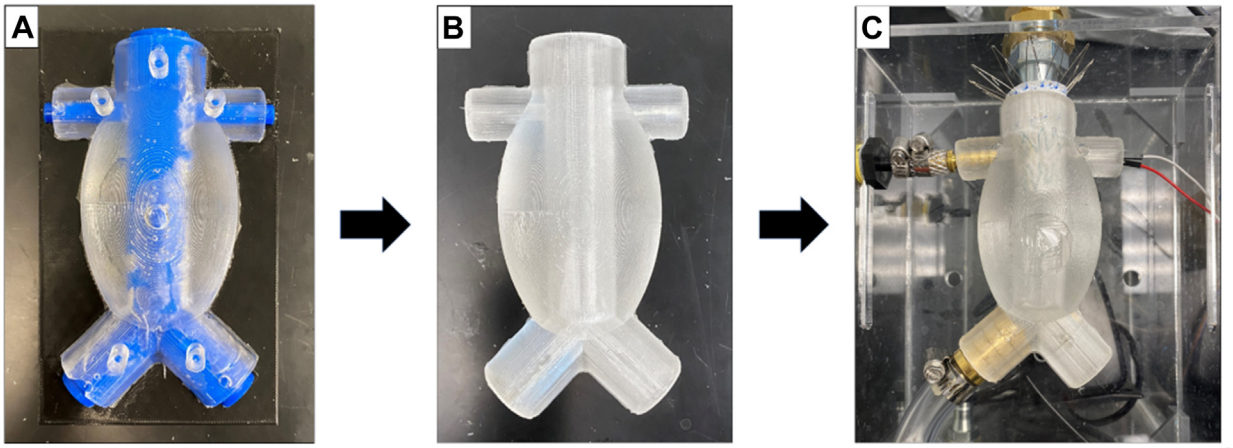

Fig 3. (A) Mold of the AAA model with the dissolvable inner core visible. **(B)** Mold of the AAA model with the inner core dissolved, leaving only the silicone shell. **(C)** The AAA phantom model has an endograft placed on the superior end, an infrared emitter on the renal artery, and is connected to the flow loop.

a rate of 60 pulses/second. These parameters were selected based on the surgeon's recommendation and the literature.[23,24] The porcine aorta was then cryosectioned, and images were taken with a microscope to determine the laser's penetration depth and whether damage occurred to the aorta.

ISF within an in vitro AAA model. For the next part of this study, we aimed to determine if the EOrD deviec could accurately detect and fenestrate an endograft within the AAA phantom model. A new probe was designed with smaller fiber optic cables than the prior tests to reduce the total surface area of the probe head. The probe head was attached to an existing 10F Aptus Endosystems TourGuide steerable catheter (Fig 4, *A*) (Medtronic Inc., Minneapolis, MN). The probe head had an outer diameter of 5.5 mm, designed to be slightly smaller than the opening of a renal artery. Its inner diameter was 3.4 mm to fit the steerable catheter. The probe head included eight channels to fit eight cables of 0.22 numerical aperture, 400-μm diameter fiber optic cables (Fig 4, *B* and *C*). The cables were cut at a length of 2 feet to achieve enough reach for deployment.

A Zenith endograft was deployed into the AAA phantom model, and the AAA phantom was hooked up to the custom flow loop chamber with the right side iliac left unattached to allow for deployment of the device. The device was deployed through the right iliac and steered towards the right-side renal artery opening. The laser probe was delivered through the steerable catheter sheath and used to fenestrate the endograft at the same settings from Measuring factor of safety for mechanical puncture method of fenestration. The device was deployed blindly four times (n = 4), and four fenestrations were created. An analysis was done to calculate the distance that the centroid of the fenestration was from the centroid of the artery opening.

Statistical analyses. Statistical analysis was performed with Prism 9 (Graphpad, La Jolla, CA). A two-tailed unpaired *t* test was used to compare the average intensity and mean max intensity between the fiber optics in air and blood. The same unpaired *t* test was conducted on the maximum force values generated from the mechanical puncture tests.

RESULTS

Testing in the blood led to a significant drop in the mean of the average intensity values from the fixed area of each fiber optic cable compared with air (99.1 ± 10.5 vs 37.58 ± 12.0; $P < .0001$) (Fig 5, *A*). The mean maximum intensity also dropped significantly from air to blood (255 ± 0.00 vs 163.3 ± 71.2; $P = .035$) (Fig 5, *B*). With a significant decrease in intensity, we still found that infrared light could be visualized through the Zenith graft material when submerged in blood. The images created from the sweep over the opening also showed that the fibers could clearly identify the top and bottom edges of the opening. The image feed from the MATLAB code did not produce a signal (ie, it gave a black screen) when facing the 3D printing resin wall, indicating no artery detection until one of the six cables met the orifice's boundaries.

The needle punctured through all tests for the mechanical fenestration test successfully. A schematic for the punctures can be seen in Fig 6, *A*. Fig 6, *B*, shows the maximum force recorded for each configuration. The mean maximum force for piercing through the endograft, porcine aorta, and endograft plus porcine aorta were −0.218 ± 0.039 lbf, −0.249 ± 0.031 lbf, −0.298 ± 0.021 lbf, respectively. The negative numbers are indicative of a compressive force. There is no significance in the difference in force values between the three groups (endograft vs porcine aorta, $P = .543$; endograft vs endograft + porcine aorta, $P = .051$; porcine aorta vs endograft and porcine

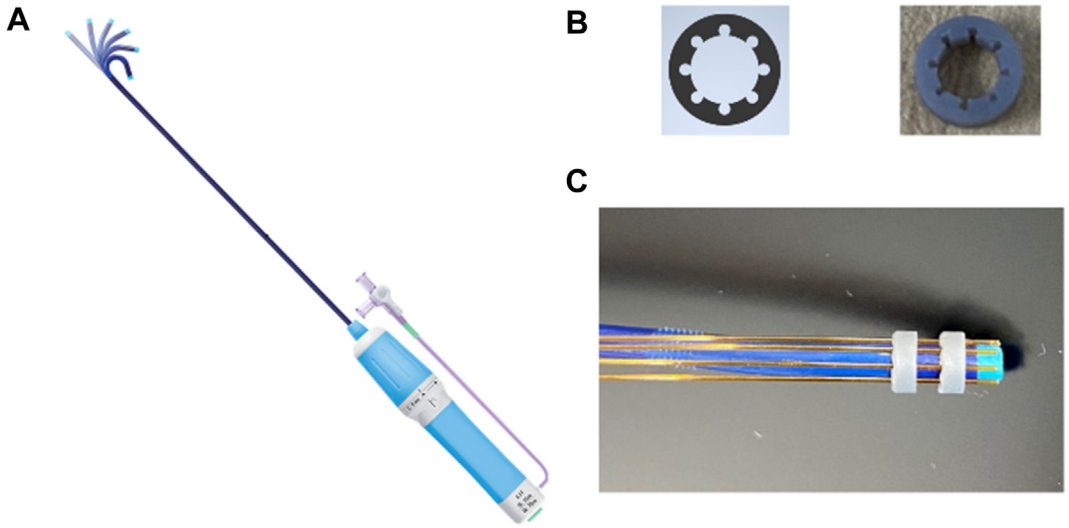

Fig 4. **(A)** Medtronic APTUS steerable sheath. **(B)** Precise 3D printed rings used to contrict the fiber optic cables to the sheath. **(C)** The fiber optic cables radially distributed around the steerable sheath.

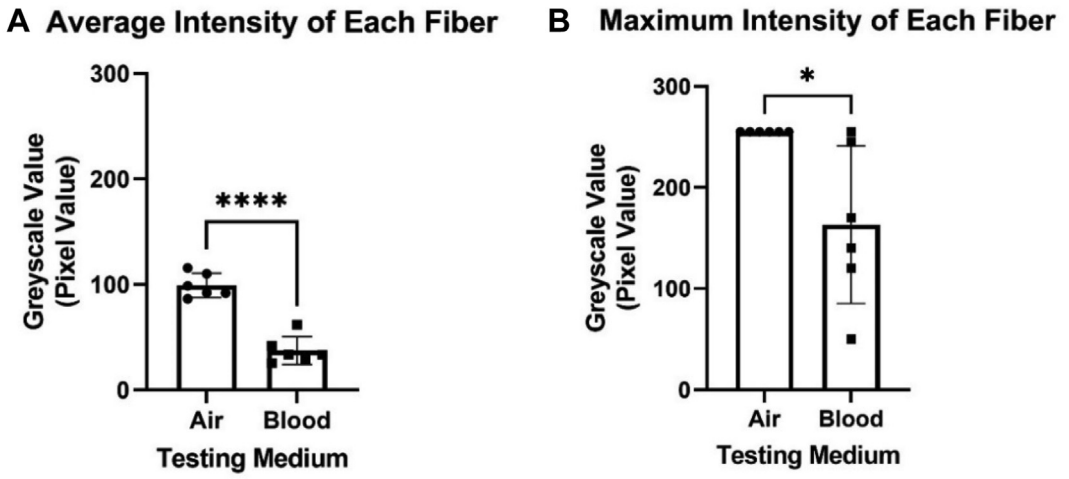

Fig 5. **(A)** Comparison of the average intensity emitted by each of the six fibers in air and in blood (****$P < .0001$). **(B)** Comparison of the maximum intensity visualized from each fiber in air and in blood.

aorta, $P = .315$). The factor of safety for the maximum force of the combination of endograft and aorta as related to the maximum force of the aorta equaled 1.20.

Both the Medtronic and the Zenith grafts were successfully laser fenestrated in 1- to 4-second pulse intervals (Fig 7, *A-D*). The imaging results from the laser penetration depth test can be seen in Fig 7. The initial thickness of each material was recorded as 0.62 mm, 2.10 mm, and 2.63 mm for the endograft, porcine aorta, and endograft, respectively. The depth of burn from the laser in the porcine aorta is 0.043 mm, 0.034 mm, 0.015 mm, and 1.56 mm for 1- through 4-second intervals, respectively. These burn depths equate to 2.0%, 1.6%, 0.7%, and 74.3% burn through the thickness of the aorta.

The AAA phantom model and custom flow loop chamber were created successfully, and four successful fenestrations were completed in the AAA phantom model. The step-by-step process for targeting the orifice to fenestration can be seen in Fig 8, *A-D*. Each time, the laser was activated for 2 seconds, and in each of the four cases, the probe created a fenestration within the boundaries of the opening. The mean distance from the centroid of the fenestration to the centroid of the artery opening was 1.450 ± 0.876 mm.

DISCUSSION

This study aimed to determine an efficient method for locating visceral artery openings for ISF. Fiber optic

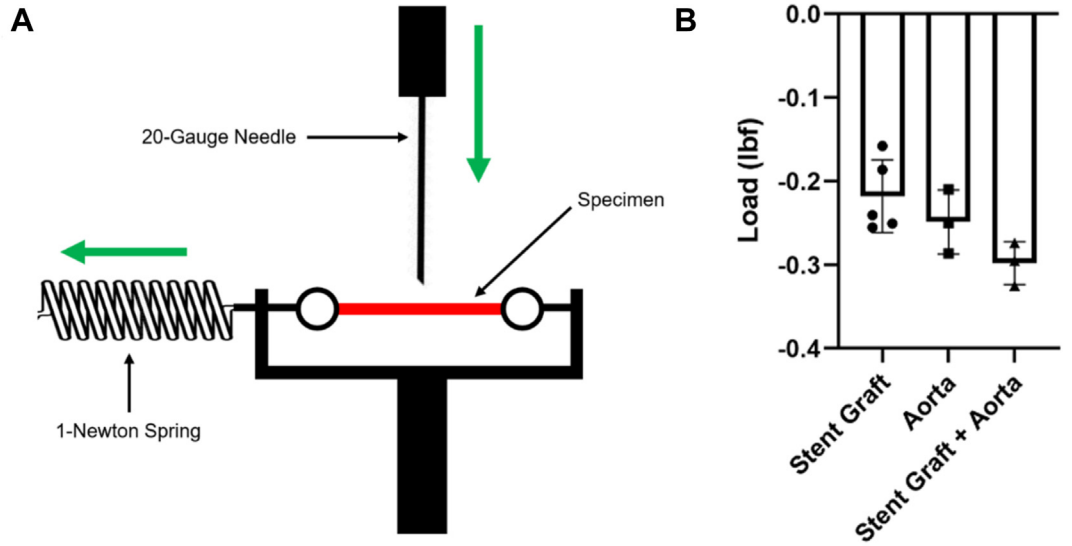

Fig 6. (A) The experimental setup where the 20G needle is lowered at a rate of 3 mm/min until piercing through the specimen. **(B)** The peak compression force (lbf) when puncturing an endograft, porcine aorta, and combination of both.

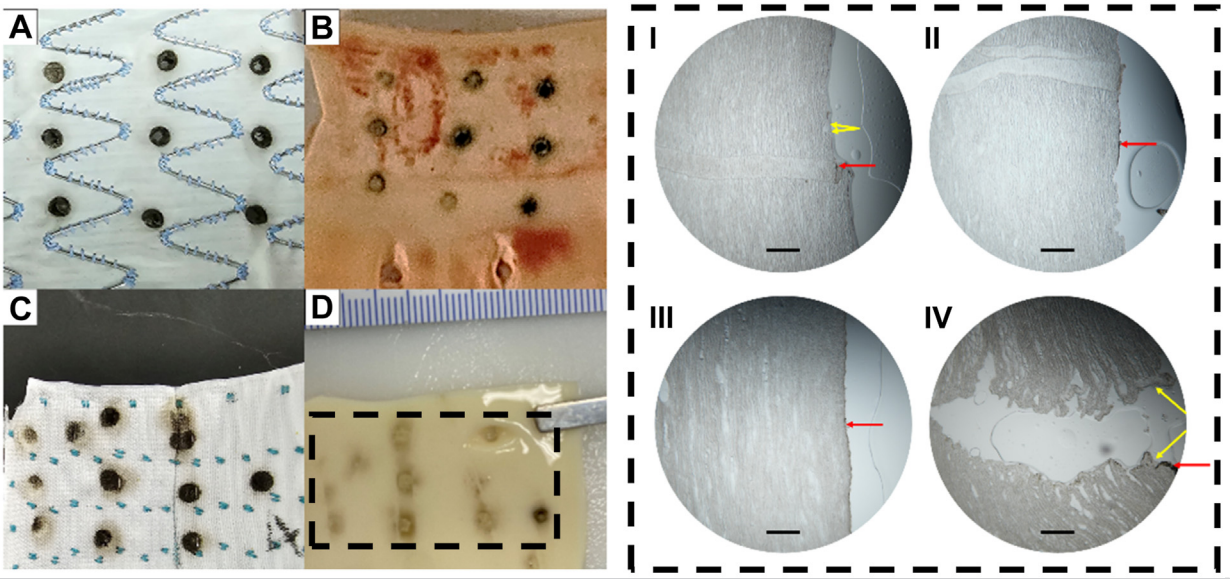

Fig 7. (A) Fenestrations through a Medtronic endograft. The laser was pulsed 1, 2, and 3 seconds for each column three times. **(B)** The markings of the laser fenestration on the porcine aorta after penetration (corresponding with **A**). **(C)** Fenestrations through a Cook Medical endograft. Each column corresponding with the time (seconds). **(D)** The porcine aorta after performing laser fenestration (from **C**). Cryosection images of the burn depths from the laser probe corresponding with **(D)**. The red arrows denote the burn markings on the lumen of the porcine aorta and the yellow arrows denote the beginning of the tissue damage that the tissue experienced. The black scale bars for each image are 200 μm.

cables coupled with a light source proved to be an effective tool for finding a model branch artery orifice, and laser fenestration emerged as the safer option for creating a hole in the graft. The experiments indicated that fiber optics could identify the boundaries of an orifice successfully using light emitted from an infrared and white light LED. Notably, the fibers displayed an ability to detect the infrared light even through the obstruction of blood and endograft material. The safety factor of 1.20 for the combination of materials to porcine aorta indicates that the force to pierce the combination of endograft and aorta is slightly higher than that of the

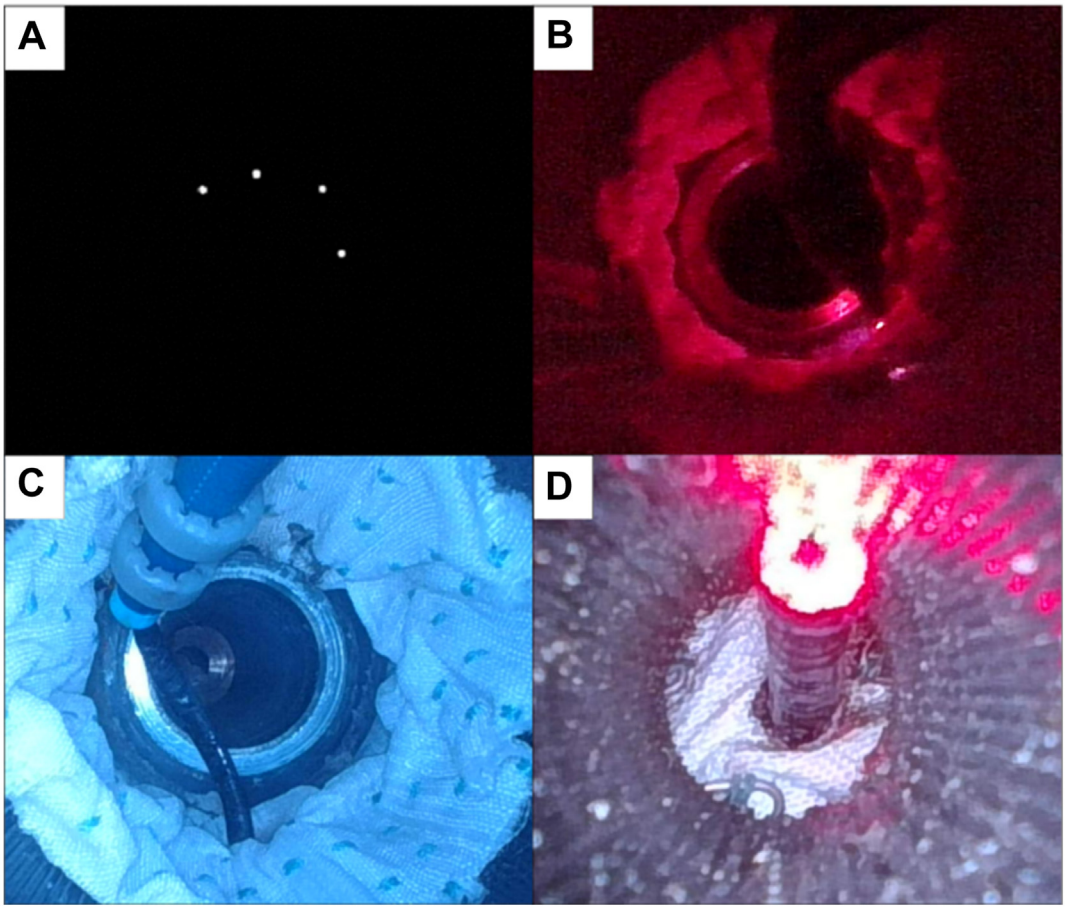

Fig 8. **(A)** The clinician's view of four fiber optic cable ends lit up, indicating a positive target. **(B)** The laser probe emerging from the steerable sheath and fenestration occurred through the endograft material. **(C)** The endovascular orifice detection (EOrD) prototype was partially removed and **(D)** the laser probe created a fenestration in the correct location. The image was taken from the visceral artery to the stent graft material.

aorta alone; therefore, the threshold for error for mechanical fenestration is small. Caution should be taken when using a needle for fenestration because the needle could pierce the aortic tissue easily through the endograft. The laser fenestration results were promising, showing that the laser could pierce the graft material at a 1-second pulse without affecting the tissue underneath the endograft substantially. Caution should be taken pulsing the laser for >3 seconds, as in the 4-second interval, the laser burned through nearly 75% of the aorta. Further work would have to be done to determine if the hole generated is satisfactory for the deployment of branching stent grafts after fenestration expansion using a balloon catheter. It was also determined that the fibers could lead to an accurate fenestration of the endograft when deployed in a AAA model. In each case, the fibers were able to locate the artery opening accurately, and the laser created a fenestration in the correct location.

Although fiber optics have been considered in other medical applications, namely, their use for endoscopes, this work is the first, to our knowledge, in which they have been explored for use in locating branch arterial orifices during ISF. Our findings suggest that fiber optics can play a significant role in this process. Digital subtraction angiography is a commonly used method for performing ISF, where a contrast agent is injected into the bloodstream, and radiographs are taken. The contrast agent helps to visualize the blood vessels, aiding in locating the arteries; however, this method provides a two-dimensional visualization, which is not sufficient for many cases of ISF. There are two main methods of performing ISF, either retrograde or antegrade. Retrograde ISF refers to fenestration from the outside of the endograft by following the path of the branching vessel. This method is considered much less complex, especially for thoracic aneurysm procedures, because a small incision can be made into the aortic arch arteries.[25] However, for abdominal aortic procedures, this method cannot typically be used because it requires much more extensive and deeper surgical incisions to locate the visceral arteries, so an antegrade approach is taken, where the fenestration is done from inside the lumen of the

aorta.[25,26] Although the success rate of antegrade ISF in the abdominal region is high,[27,28] there are minimal clinical reports for antegrade ISF owing to the complexity of targeting the opening of the visceral arteries and the limited technology available. Methods of more efficiently locating arteries without the use of high-intensity imaging and for emergency cases are needed. The findings in this study build toward the development of a potential solution for cases using antegrade ISF.

W. L. Gore & Associates received approval in January of 2024 from the US Food and Drug Administration for their new device, the Gore Excluder Thoracoabdominal Branch Endoprosthesis. The Gore Excluder Thoracoabdominal Branch Endoprosthesis is designed to be an off-the-shelf endograft for complex aneurysm repair, an alternative to open repair. The device contains four precut ports, used to cannulate two visceral arteries and two renal arteries, which will be used for deploying branching stent grafts.[29] No patients died after a 30-day follow-up from the procedure; however, 31% had significant blood loss owing to the operation.[30] The long-term results of the clinical trials have not yet been published. Currently, this device still does not offer customizability for differing complex aneurysm geometries and has very strict indications for use (IFU). The device also boasts a large cost to the insitution. The main advantages of our EOrD device is that it can be used on off-the-shelf endovascular grafts, it is a cheaper alternative for complex AAA repair, and it is a solution for patients that do not fall into the IFU of PMEGs or CMDs.

This study has its limitations. The early design iterations have focused primarily on assessing feasibility rather than aligning perfectly with the specific sizes essential to the prototype's final development. In easing the manufacturing process and ensuring smooth experimentation, the dimensions of the test benches and probes we used were deliberately larger than their physiological counterparts. The anatomy of individuals can significantly differ in terms of complexity and actual dimensions. The benchmarks set in this study might not accurately mirror the intricacies of human anatomy. The in vitro phantom test was only conducted in air. We have yet to determine if accurate fenestrations can be made with blood flowing through the phantom; however, the blood test we completed leads us to believe that it will be possible.

The EOrD device is intended to offer an alternative to current costly and time consuming approaches to complex AAA repair. While the initial results are promising, there is still much work to be done. Future studies will include the design of a smaller prototype for testing the device in more realistic AAA phantoms and cadavers. A custom miniaturized probe will be designed using fiber optic wires with a smaller diameter of 200 μm. The smaller diameter fiber enables the addition of more fibers to the probe head without adding rigidity to the steerable catheter. Manufacturing a custom steerable sheath will help in producing a device that fits our exact needs, including directly embedding the fiber optic cables within the steerable catheter. Additional patient-specific AAA phantom models will be developed for more accurate in vitro testing. Finally, the continuation in the development of the custom flow loop to create a pulsatile flow of both water and blood within the AAA phantom model is needed to fully understand the capabilities of the EOrD device and its IFU.

CONCLUSIONS

This study presents the first step in enabling ISF locally by detecting the orifice of the visceral arteries from the lumen of the endograft. The introduction of a technique that reduces the need for high-radiation angiograms and long wait times for custom-made grafts is a step in improving the repair of complex AAAs. The EOrD device has the potential to cut operation time and cost. It also offers the possibility of immediate surgeries in emergent complex AAA cases. The results also extend beyond just the specific procedure for which we proposed the device. Our research opens the door for advancements in repairing ascending thoracic aneurysms, the treatment of traumatic aortic injuries, and the emergent repair of aortas (aneurysm rupture and other trauma events).

FUNDING

Funded by the National Institutes of Health HL157646 and the Michael G. Wells Foundation for the funds to perform the feasibility studies that led to US patent application US17/603,881.

DISCLOSURES

None.

REFERENCES

1. Vorp DA. Biomechanics of abdominal aortic aneurysm. *J Biomech*. 2007;40:1887–1902.
2. Brown LC, Powell JT. Risk factors for aneurysm rupture in patients kept under ultrasound surveillance. *Annals of surgery*. 1999;230:289.
3. Lederle FA, Wilson SE, Johnson GR, et al. Immediate repair compared with surveillance of small abdominal aortic aneurysms. *N Engl J Med*. 2002;346:1437–1444.
4. Kühnl A, Erk A, Trenner M, Salvermoser M, Schmid V, Eckstein HH. Incidence, treatment and mortality in patients with abdominal aortic aneurysms: an analysis of hospital discharge data from 2005–2014. *Dtsch Ärztebl Int*. 2017;114:391.
5. Wilmink A, Quick CG. Epidemiology and potential for prevention of abdominal aortic aneurysm. *Br J Surg*. 1998;85:155–162.
6. Conrad MF, Crawford RS, Pedraza JD, et al. Long-term durability of open abdominal aortic aneurysm repair. *J Vasc Surg*. 2007;46:669–675.
7. Parodi JC. Endovascular repair of abdominal aortic aneurysms and other arterial lesions. *J Vasc Surg*. 1995;21:549–557.
8. Greenhalgh R, The E. Comparison of endovascular aneurysm repair with open repair in patients with abdominal aortic aneurysm (EVAR trial 1), 30-day operative mortality results: randomised controlled trial. *Lancet*. 2004;364:843–848.
9. Li Y, Hu Z, Bai C, et al. Fenestrated and chimney technique for juxtarenal aortic aneurysm: a systematic review and pooled data analysis. *Sci Rep*. 2016;6:1–12.
10. Melo RG, Prendes CF, Caldeira D, et al. Systematic review and meta-analysis of physician modified endografts for treatment of thoraco-

abdominal and complex abdominal aortic aneurysms. *Eur J Vasc Endovasc Surg*. 2023;65.5:e78.
11. Oderich GS, Forbes TL, Chaer R, et al. Reporting standards for endovascular aortic repair of aneurysms involving the renal-mesenteric arteries. *J Vasc Surg*. 2021;73(1S):4S–52S.
12. Oderich GS, Greenberg RK, Farber M, et al. Results of the United States multicenter prospective study evaluating the zenith fenestrated endovascular graft for treatment of juxtarenal abdominal aortic aneurysms. *J Vasc Surg*. 2014;60:1420–1428.e5.
13. Ricotta JJ II, Tsilimparis N. Surgeon-modified fenestrated-branched stent grafts to treat emergently ruptured and symptomatic complex aortic aneurysms in high-risk patients. *J Vasc Surg*. 2012;56:1535–1542.
14. Swerdlow NJ, Wu WW, Schermerhorn ML. Open and endovascular management of aortic aneurysms. *Circ Res*. 2019;124:647–661.
15. Katsargyris A, Uthayakumar V, de Marino PM, Botos B, Verhoeven EL. Aneurysm rupture and mortality during the waiting time for a customised fenestrated/branched stent graft in complex endovascular aortic repair. *Eur J Vasc Endovasc Surg*. 2020;60:44–48.
16. Gallitto E, Faggioli G, Spath P, et al. The risk of aneurysm rupture and target visceral vessel occlusion during the lead period of custom-made fenestrated/branched endograft. *J Vasc Surg*. 2020;72:16–24.
17. Dossabhoy SS, Simons JP, Flahive JM, et al. Fenestrated endovascular aortic aneurysm repair using physician-modified endovascular grafts versus company-manufactured devices. *J Vasc Surg*. 2018;67:1673–1683.
18. Boufi M, Alexandru G, Tarzi M, et al. Systematic review and meta-analysis of ex-situ and in-situ fenestrated stent-grafts for endovascular repair of aortic arch pathologies. *J Endovasc Ther*. 2024;31:1041–1051.
19. Ye K, Qiu P, Qin J, et al. Internal iliac artery preservation during endovascular aortic repair using in situ laser fenestration. *J Vasc Surg*. 2023;77:129–135.
20. Le Houérou T, Álvarez-Marcos F, Gaudin A, et al. Midterm outcomes of antegrade in situ laser fenestration of polyester endografts for urgent treatment of aortic pathologies involving the visceral and renal arteries. *Eur J Vasc Endovasc Surg*. 2023;65:720–727.
21. Glorion M, Coscas R, McWilliams R, Javerliat I, Goëau-Brissonniere O, Coggia M. A comprehensive review of in situ fenestration of aortic endografts. *Eur J Vasc Endovasc Surg*. 2016;52:787–800.
22. Redlinger RE Jr, Ahanchi SS, Panneton JM. In situ laser fenestration during emergent thoracic endovascular aortic repair is an effective method for left subclavian artery revascularization. *J Vasc Surg*. 2013;58:1171–1177.
23. DiBartolomeo AD, Han SM. Techniques of antegrade in situ laser fenestration for endovascular aortic repair of complex abdominal and thoracoabdominal aortic aneurysms. *J Vasc Surg Cases Innov Tech*. 2022;8:787–793.
24. Wang Y, Downie S, Wood N, Firmin D, Xu XY. Finite element analysis of the deformation of deep veins in the lower limb under external compression. *Med Eng Phys*. 2013;35:515–523.
25. Piazza R, Carbone M, Berchiolli RN, Ferrari V, Ferrari M, Condino S. A systematic review on methods and tools for the in situ fenestration of aortic stent-graft. *IEEE Rev Biomed Eng*. 2021;16:348–356.
26. Tse LW, Bui BT, Lerouge S, et al. In vivo antegrade fenestration of abdominal aortic stent-grafts. *J Endovasc Ther*. 2007;14:158–167.
27. Leger T, Tacher V, Majewski M, Touma J, Desgranges P, Kobeiter H. Image fusion guidance for in situ laser fenestration of aortic stent graft for endovascular repair of complex aortic aneurysm: feasibility, efficacy and overall functional success. *Cardiovasc Intervent Radiol*. 2019;42:1371–1379.
28. Le Houérou T, Fabre D, Alonso CG, et al. In situ antegrade laser fenestrations during endovascular aortic repair. *Eur J Vasc Endovasc Surg*. 2018;56:356–362.
29. Cambiaghi T, Grandi A, Bilman V, Melissano G, Chiesa R, Bertoglio L. Anatomic feasibility of the investigational GORE EXCLUDER thoracoabdominal branch endoprosthesis (TAMBE), off-the-shelf multibranched endograft for the treatment of pararenal and thoracoabdominal aortic aneurysms. *J Vasc Surg*. 2021;73:22–30.
30. Oderich GS, Farber MA, Silveira PG, et al. Technical aspects and 30-day outcomes of the prospective early feasibility study of the GORE EXCLUDER thoracoabdominal branched endoprosthesis (TAMBE) to treat pararenal and extent IV thoracoabdominal aortic aneurysms. *J Vasc Surg*. 2019;70:358–368.e6.

Submitted Jun 25, 2024; accepted Oct 14, 2024.